Geomorphic evidence for post-10 Ma uplift of the western flank of the central Andes 18°30′–22°S

Gregory D. Hoke,[1,2] Bryan L. Isacks,[1] Teresa E. Jordan,[1] Nicolás Blanco,[3] Andrew J. Tomlinson,[3] and Jahandar Ramezani[4]

Received 14 November 2006; revised 4 April 2007; accepted 11 June 2007; published 31 October 2007.

[1] The western Andean mountain front forms the western edge of the central Andean Plateau. Between 18.5° and 22°S latitude, the mountain front has ~3000 m of relief over ~50 km horizontal distance that has developed in the absence of major local Neogene deformation. Models of the evolution of the plateau, as well as paleoaltimetry estimates, all call for continued large-magnitude uplift of the plateau surface into the late Miocene (i.e., younger than 10 Ma). Longitudinal river profiles from 20 catchments that drain the western Andean mountain front contain several streams with knickpoint-bounded segments that we use to reconstruct the history of post-10 Ma surface uplift of the western flank of the central Andean Plateau. The generation of knickpoints is attributed to tectonic processes and is not a consequence of base level change related to Pacific Ocean capture, eustatic change, or climate change as causes for creating the knickpoint-bounded stream segments observed. Minor valley-filling alluvial gravels intercalated with the 5.4 Ma Carcote ignimbrite suggest uplift related river incision was well under way by 5.4 Ma. The maximum age of river incision is provided by the regionally extensive, approximately 10 Ma El Diablo–Altos de Pica paleosurface. The river profiles reveal that relative surface uplift of at least1 km occurred after 10 Ma.

Citation: Hoke, G. D., B. L. Isacks, T. E. Jordan, N. Blanco, A. J. Tomlinson, and J. Ramezani (2007), Geomorphic evidence for post-10 Ma uplift of the western flank of the central Andes 18°30′–22°S, *Tectonics*, *26*, TC5021, doi:10.1029/2006TC002082.

1. Introduction

[2] The processes and rates related to the formation of large continental plateaus remain controversial. Many different mechanisms and ideas have been invoked to explain their evolution, spanning climatic controls [e.g., *Montgomery et al.*, 2001], pure structural thickening via horizontal shortening [e.g., *McQuarrie*, 2002], to viscous flow of lower crustal material [*Clark and Royden*, 2000]. The outcomes of some models of plateau forming processes are much easier to test with observation than others. The simplest metric of tectonic activity is upper crustal deformation combined with chronologic constraints. In contrast, proposed mechanisms of plateau formation not resulting in surface-breaking faults are much more difficult to constrain.

[3] The Andes of South America are home to the central Andean Plateau, the second highest continental plateau on Earth at ~4 km average elevation. The plateau is bounded on either side by mountainous topography of the Eastern and Western Cordilleras. The eastern side of the Andean orogen is characterized by a wide belt of Neogene supracrustal deformation expressed by numerous surface-breaking faults and folds. The belt has varied tectonic style, typified by basement uplifts in the Argentine and Peruvian forelands, as well as the spectacular thin-skinned Sub-Andean fold-and-thrust belt in Bolivia. Structural studies indicate that as much as 300 km of Neogene horizontal shortening [*McQuarrie et al.*, 2005] has occurred across the entire plateau and postulate that it generated 3000–4000 m of relief between the plateau and the undeformed foreland [*Elger et al.*, 2005]. By contrast, the western mountain front of the central Andes contains a similar amount of relief but only minor Neogene supracrustal deformation (Figure 1). Several studies related to the development of the plateau or the central Andes as a whole [*Garzione et al.*, 2006; *Gregory-Wodzicki*, 2000; *Isacks*, 1988; *Kay and Kay*, 1993; *Kay et al.*, 1994; *Lamb and Hoke*, 1997] postulate that uplift of the plateau surface occurred throughout the Miocene. However, the western mountain front has provided little evidence in support of the uplift history interpretations that were based on observations from other parts of the plateau, due to the lack of well-defined geologic structures of appropriate age. Where structural geology approaches cannot be applied, we must explore other methods to test the various hypotheses for plateau formation. Here we examine the longitudinal stream profiles from 20 drainage networks (Figure 1) descending the western flank of the central Andean Plateau in an effort to detect and quantify post-10 Ma relief formation in the region. To do so we perform three tasks. The first is the extraction of stream profiles from digital elevation data, the second is

[1]Department of Earth and Atmospheric Sciences, Cornell University, Ithaca, New York, USA.
[2]Now at Department of Earth and Environmental Sciences, University of Rochester, Rochester, New York, USA.
[3]Servicio Nacional de Geología y Minería, Santiago, Chile.
[4]Department of Earth Atmospheric and Planetary Sciences, Massachusetts Institute of Technology, Cambridge, Massachusetts, USA.

Copyright 2007 by the American Geophysical Union.
0278-7407/07/2006TC002082

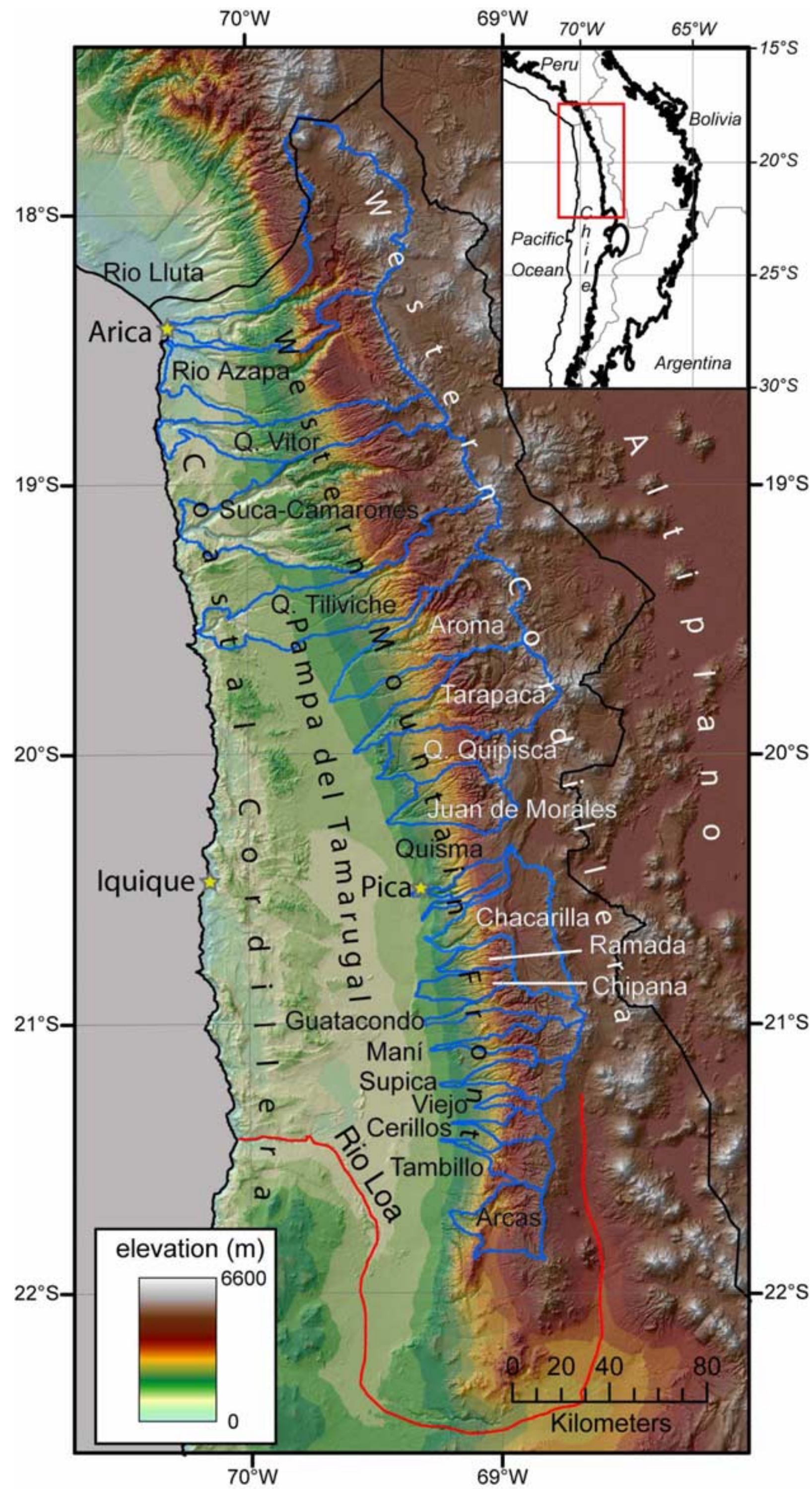

Figure 1. Shaded relief topographic image with the locations of the major physiographic elements of the western Andes of northernmost Chile and names of the 20 basins considered in this study. Country boundaries are shown with light gray lines. The towns of Iquique, Pica, and Arica are labeled for reference. Between the Quebrada de Tiliviche and Río Loa, all of the drainage basins are closed or effectively closed. The location of the Río Loa is labeled in red. Inset shows the location of the study area, political boundaries, country names, and the central Andean Plateau delineated by the 3000 m elevation contour (thick line).

demonstration of the ages of stream segments, and third is reconstruction of the surface relief at the times when the dated stream segments were created.

2. Geologic Setting

[4] The Andes are the type example of a noncollisional orogen in a convergent margin setting. Here the Nazca plate subducts below the overriding South American plate. Subduction along this margin has been active since the Mesozoic, with the modern phase of mountain building beginning in the latest Oligocene [*Jordan et al.*, 1997; *Mpodozis and Ramos*, 1989]. The central Andean segment of the orogen is dominated by the central Andean Plateau which spans some ~1500 km N-S and 300 km E-W at its widest point. It is bounded to the west by the volcanic peaks of the Western Cordillera (the volcanic arc) and to the east by the Eastern Cordillera (the hinterland of the modern Sub-Andean fold-thrust belt).

[5] Our study area lies within the modern Andean fore arc and forms the western flank of the central Andean Plateau. Several physiographic provinces exist in the study area (Figure 1). From west to east, they are the (1) Coastal Cordillera, (2) Central Depression (Pampa del Tamarugal), (3) western mountain front, (4) Western Cordillera, and (5) Altiplano (Figure 1). In the study area the Coastal Cordillera lies between the Pacific Ocean and the Central Depression and has peaks as high as 2500 m and an average elevation of ~1500 m that wanes toward the north, where it is less than 1000 m at 18.5°S. The Coastal Cordillera is composed of Mesozoic volcanic arc and plutonic rocks, and marine sedimentary rocks, with Oligocene to Recent alluvial and colluvial sedimentary units filling intermontane basins [*García et al.*, 2004; *Muzzio*, 1986, 1987; *Servicio Nacional de Geología y Minería* (*SERNAGEOMIN*), 2002; *Silva*, 1977]. The Central Depression is a broad plain at ~1000 m elevation that lies between the Coastal Cordillera and the western mountain front and is underlain by Oligocene to Recent sedimentary fill. The western mountain front connects the high elevations of the Western Cordillera and Altiplano to the Central Depression. The Western Cordillera is composed of rocks of the Miocene to Recent volcanic arc.

[6] All parts of the study area below 3500 m elevation are subject to the hyperarid conditions of the Atacama Desert. The analysis of meteorological station data by *Houston and Hartley* [2003] shows that rainfall is strongly dependent on elevation in this area. At 1000 m, in the Central Depression, rainfall is <50 mm/yr, though at elevations >3500 m, rainfall is ~150 mm/yr. The high peaks of the Western Cordillera (5000–6000 m) do not have station data but are believed to have annual precipitation in excess of 200 mm/yr. Several lines of evidence point to the long-term stability of climate in this region [*Alpers and Brimhall*, 1988; *Houston and Hartley*, 2003; *Sillitoe and McKee*, 1996].

[7] The western mountain front in northernmost Chile is a steep (~3°) topographic front with ~3000 m of vertical relief occurring over ~50 km horizontal distance. The latest Oligocene middle Miocene sedimentary package exposed along the front is broadly deformed into a west dipping monoclinal form [*Isacks*, 1988; *Mortimer et al.*, 1974; *Mortimer and Saric Rendic*, 1975] (Figure 2), with several distinct sedimentary and volcanic units creating marker horizons that are continuous from the crest of the mountain front to its toe. Locally, parts of this sequence are folded and cut by steeply dipping west vergent reverse faults that are estimated to have produced 3–8 km of horizontal shortening [*Digert et al.*, 2003; *Farías et al.*, 2005; *García*, 2002; *García et al.*, 2004; *Muñoz and Charrier*, 1996; *Pinto et al.*, 2004; *Victor et al.*, 2004]. Currently, two competing models exist for the topographic relief development of the western Andean mountain front. *Isacks*' [1988] model interprets the upper crust as a monoclinal flexure that is an accommodation structure between the rising plateau and the static fore arc [*Isacks*, 1988]. An alternative contends that offset on upper crustal faults generates the full topographic relief [*Muñoz and Charrier*, 1996; *Victor et al.*, 2004]. Although the two opposing models lead to the same basic geometry and end result of the western monocline as a landform, there are differences in both the mechanisms and timing of uplift. In *Isacks*' [1988] model, excluding the thermal effects, uplift is a result of isostatic adjustment to thickening in the plateau caused by east-west shortening across the orogen. In this model, deformation along the western mountain front, in particular the monoclinal flexure, does not play an important role in the structural shortening but instead accommodates the difference in isostatic compensation between the undeformed fore arc and the deforming plateau, and as such, the flexure is a consequence rather than a cause of uplift. Because the model links uplift to shortening history across the orogen, it predicts that formation of the western mountain front occurred throughout the time span of shortening, hence throughout the Miocene to Recent [*Allmendinger et al.*, 1997; *Isacks*, 1988]. In the fault based model, the faulting and folding are the cause and not the consequence, of uplift. Therefore the model predicts that relief generation is restricted to the timing of the local faults and folds [*Farías et al.*, 2005; *Muñoz and Charrier*, 1996; *Victor et al.*, 2004].

[8] The profound and long-term aridity of this region results in the extraordinary preservation of strata on the steep western mountain front, as well as an extremely well preserved poly phase landscape [*García and Hérial*, 2005; *Hoke et al.*, 2004; *Mortimer and Saric Rendic*, 1975; *Tosdal et al.*, 1984; *Worner et al.*, 2002] (Figures 2 and 3). The Neogene cover of the western mountain front is composed mostly of alluvial sedimentary rocks with intercalated tuffs ranging from the latest Oligocene to Pliocene age. These units are north of 19.75°S, the Oligo-Miocene Oxaya Formation [*García*, 2002; *Salas et al.*, 1966] and overlying middle Miocene El Diablo Formation; and south of 19.75°S, the Oligo-Miocene Altos de Pica Formation [*Galli Olivier and Dingman*, 1962] (Figure 3) and overlying uppermost Miocene–lower Pliocene strata. These units and several of their exposed members create regionally extensive, recognizable surfaces that can be used as time-

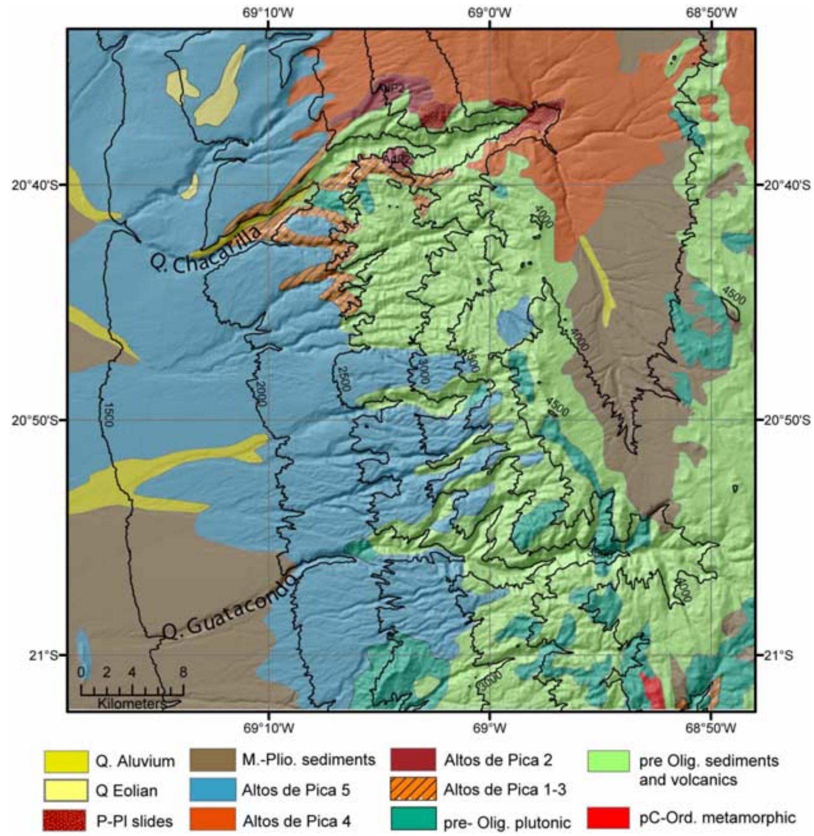

Figure 2. Geologic map modified from the 1:1,000,000 geologic map of Chile [*SERNAGEOMIN*, 2002] of the area between Quebradas Chacarilla and Maní draped over the shaded relief topography of the SRTM 90 m DEM. The elevation of the SW corner of the map is ~1200 m, while the northeast corner is at 4000 m. The 500 m contours on the map show the monoclinal form of the western mountain front and the relatively undissected nature of the upper member of the Altos de Pica Formation as it extends from the lower elevations of the Pampa del Tamarugal to higher elevations to the east. The highest islands of Altos de Pica occur at elevations near 4000 m.

lines. Particularly useful in this study are the top surfaces of the El Diablo and Altos de Pica Formations.

[9] The El Diablo and Altos de Pica Formations are choronostratigraphically correlative (Figure 3) [*Farías et al.*, 2005; *García et al.*, 2004; *Pinto et al.*, 2004] and laterally contiguous units [*SERNAGEOMIN*, 2002]. On the basis of different geochronologic constraints, we treat the top surfaces of the El Diablo and Altos de Pica Formation as one continuous, temporally equivalent pediment surface. Traditionally the pediment at the top of El Diablo Formation [*Tobar et al.*, 1968] has been interpreted to be ~10 Ma, an age constrained by the ages of andesite clasts (youngest clast age of 11.9 Ma) within the top few meters of the unit [*García*, 2002; *García and Hérial*, 2005] and by the 8–9 Ma K-Ar age of the Tana lava flow which overlies the El Diablo 142 surface [*Mortimer et al.*, 1974; *Muñoz and Sepulveda*, 1992; *Pinto et al.*, 2004] (Figure 3). Likewise, new chronologic data (see auxiliary material Text S1) for ignimbrite horizons broadly bracket the age of the pediment surface at the top of the Altos de Pica Formation.[1] The pediment is older than the Carcote ignimbrite inset in river valleys incised into the pediment surface (hence older than 5.4 Ma) and younger than the youngest ignimbrite interbedded within the Altos de Pica Formation, and hence younger than 13.03 Ma (Figure 3). Further to the south, the base of the Arcas fan overlies the top surface of Altos de Pica and has an age of ~7 Ma [*Kiefer et al.*, 1997]. In contrast to the preceding, *von Rotz et al.* [2005] propose a slightly younger age, between 8.5 and 7.5 Ma, for the El Diablo Surface on the basis of magnetostratigraphy and a Rb-Sr age on an intercalated tuff near the top of the formation. Although slightly younger, their proposed age is broadly similar to the previously proposed age for the surface. ^{21}Ne cosomogenic nuclide studies attempting to date the pediment surfaces have all yielded ages that are outside of what is stratigraphically reasonable [*Dunai et al.*, 2005; *Evenstar et al.*,

[1]Auxiliary material data sets are available at ftp://ftp.agu.org/apend/tc/2006tc002082. Other auxiliary material files are in the HTML.

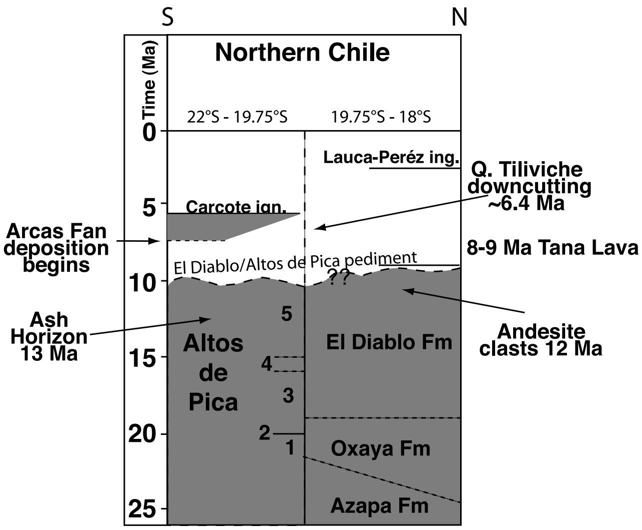

Figure 3. Generalized stratigraphy of the western Andean mountain front between 18°30′S and 22°S. Age constraints are from *Mortimer et al.* [1974] (Tana Lava), *García* [2002] (andesite clasts), *Worner et al.* [2002] (Lauca-Peréz Ignimbrite), *Kiefer et al.* [1997] (Arcas Fan), and this paper (Quebrada Tiliviche, Carcote Ignimbrite, and the 13 Ma ash horizon in Altos de Pica Formation).

2005]. No data directly constrain the age of the El Diablo Altos de Pica pediment surface.

3. Rivers of Northernmost Chile

[10] We consider rivers that drain the western mountain front of the central Andes between 18.5° and 22°S latitude (Figure 1) as potential recorders of surface uplift on the western slope of the central Andean Plateau. *Mortimer* [1980] was the first to study and describe the drainages of northern Chile. The age of the mountain front drainage systems are constrained by the fact that all of the basins are incised into the 10 Ma Altos de Pica–El Diablo pediment surface and river valleys between 20 and 22°S are partly filled by the 5.4 Ma Carcote ignimbrite (Figure 4; see auxiliary material Text S1) and therefore can be assigned a late Miocene age.

[11] Two general classes of river valleys exist in this region, those with outlets to the Pacific Ocean (rivers between 18.5° and 19.75°S and the Río Loa with its outlet at 21.5°S) and those that drain into the effectively closed Pampa del Tamarugal basin (19.75°–22°S). All of the modern drainage basins used in this study have their headwaters at elevations >4000 m. Rivers that drain to the Pacific Ocean have a maximum relief of ~6000 m, while those streams that drain into the Pampa del Tamarugal Basin have ~4500 m of relief. Figure 5 shows the representative relief structures for the two classes of drainage system.

[12] North and south of the closed Pampa del Tamarugal Basin, rivers that drain the mountain front incise the Coastal Cordillera and drain to the Pacific (Figure 1). The Río Loa and Quebrada Tilliviche river profiles have the least advanced migration of their knickpoints related to this incision event. The timing of this event for the Río Loa can be constrained by the crosscutting relationships between the valley and the local stratigraphy near the town of Quillagua [*Sáez et al.*, 1999]. Near the top of the deposits cut by the Río Loa is a 6 Ma volcanic ash [*Sáez et al.*, 1999], which can be used to infer that the initiation of incision occurred sometime after 6 Ma. Despite the fact that the Loa has captured all of the basins that drain into the Salar de Llamara, the extremely slow propagation of the knickpoint back into the Salar has thus far effectively isolated the streams which drain the western Andean slope from their new base level.

[13] The age of down cutting of the Quebrada Tiliviche across the Coastal Cordillera (Figure 1) is constrained by new geochronologic data presented here. A strath terrace cut into Mesozoic bedrock occurs at an elevation of 950 m below sea level (msl), a position that is 50 m below the top of the canyon and ~550 m above the valley bottom (Figure 6). The position of the terrace high on the canyon wall indicates it accumulated at an early stage in the incision of the canyon. U-Pb dating of zircons in a volcanic ash intercalated in the river deposits overlying the strath indicates a depositional age of 6.4 Ma. The post terrace incision rate calculated using these values is ~90 m/Ma. This incision has two possible origins, one related to a breakthrough or spillover to the Pacific Ocean and the other being related to surface uplift of the Coastal Cordillera. The breakthrough or spillover hypothesis requires that the Central Depression did not drain to the Pacific prior to the circa 6.4 Ma incision, a situation that is not consistent with the dominance of fluvial deposits and lack of evaporite deposits near the latitude of Quebrada Tiliviche. In either case, despite the circa 6.4 Ma age for initiation of down cutting, the knickpoint has only migrated 10 km into the Central Depression where river incision is minimal (see profiles of *Mortimer* [1980] and *Hoke* [2006]). In contrast, the knickpoint has already migrated through the canyons farther north to the foot of the western slope. This may suggest either that the canyons to the north have an older age than the 7.5 Ma age estimated by *Kober et al.* [2006] or that the smaller Tiliviche valley has a much lower stream power for down cutting. *Worner et al.* [2002] placed a minimum age constraint on the development of the Lluta valley with a 2.7 Ma $^{40}Ar/^{39}Ar$ age on the Lauca-Pérez ignimbrite at the bottom of the valley near its outlet to the Pacific Ocean.

4. Stream Profile Reconstruction Methodology

[14] We use knickpoint-bounded segments of river profiles to reconstruct the downstream paleoprofiles of rivers that drain the western flank of the central Andes. This approach relies on the implicit assumption that the river profile segment being modeled existed under equilibrium conditions and that knickpoints migrate upstream in erosional waves [*Whipple and Tucker*, 1999]. River profiles can serve as sensitive indicators of climate

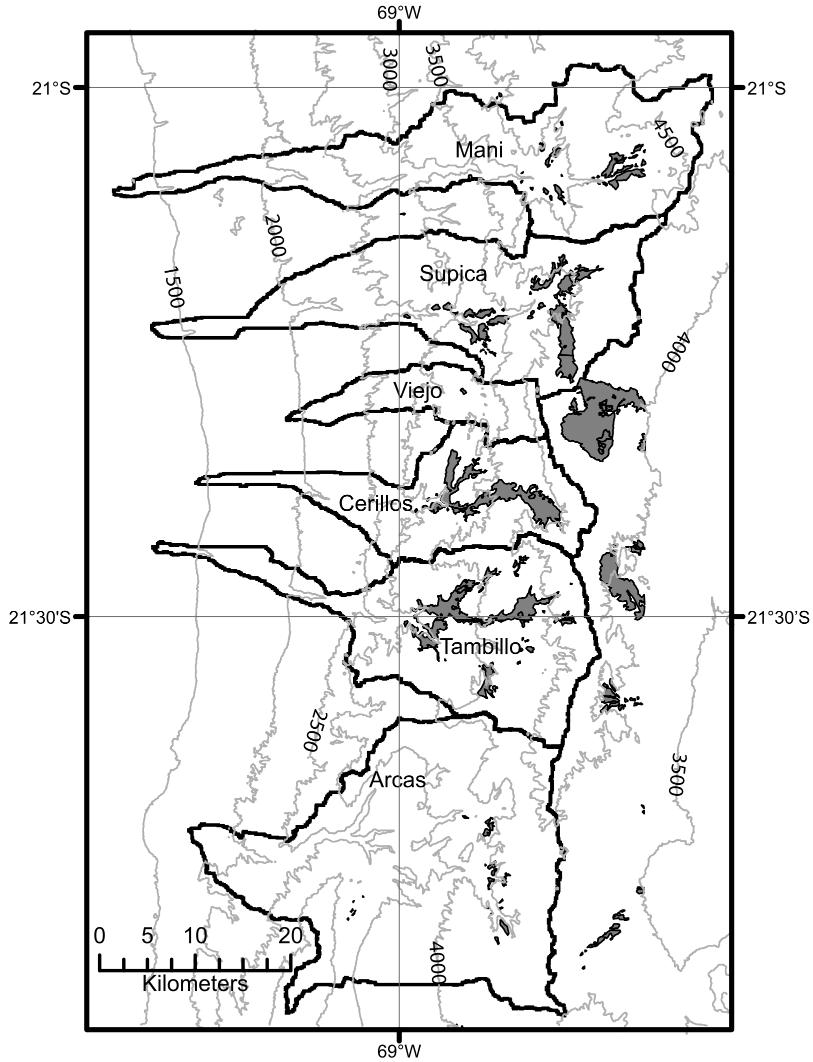

Figure 4. Distribution of the Carcote Ignimbrite (gray polygons) in the catchments (heavy black lines) that drain the southern end of the study area. Topographic contours (gray lines) are derived from 90 m SRTM data and have a 500 m spacing.

change [*Zaprowski et al.*, 2005], base level fluctuation and/or tectonic forcing [*Kirby and Whipple*, 2001; *Snyder et al.*, 2000; *Whipple and Tucker*, 1999; *Wobus et al.*, 2003]. In this paper we follow the reasoning discussed by *Snyder et al.* [2000] and *Schoenbohm et al.* [2004]. The stream power erosion model for a detachment-limited bedrock stream predicts channel erosion as a function of drainage area (A) and slope (S),

$$\varepsilon = KA^m S^n \tag{1}$$

where ε is the rate of bedrock channel erosion, K is a coefficient of erosion, and the exponents m and n are positive constants [*Whipple and Tucker*, 1999]. According to this model, slope must decrease with increasing drainage area in order to keep the rate of channel bed erosion constant. In tectonically active regions, river bed elevation through time (dz/dt) is a balance between uplift rate (U) and erosion rate ε,

$$dz/dt = U - \varepsilon = U - KA^m S^n \tag{2}$$

In the steady state (equilibrium) case where $dz/dt = 0$, (2) simplifies and can be rearranged to yield

$$S = (U/K)^{1/n} A^{-m/n} \tag{3}$$

Substitution of Hack's law, $A = x^h$ [*Hack*, 1957], where x is equal to distance downstream in meters and h is a dimensionless constant with a value of $\sim$1.6, for the area term (A) in equation (3), and integration yields the simplified version

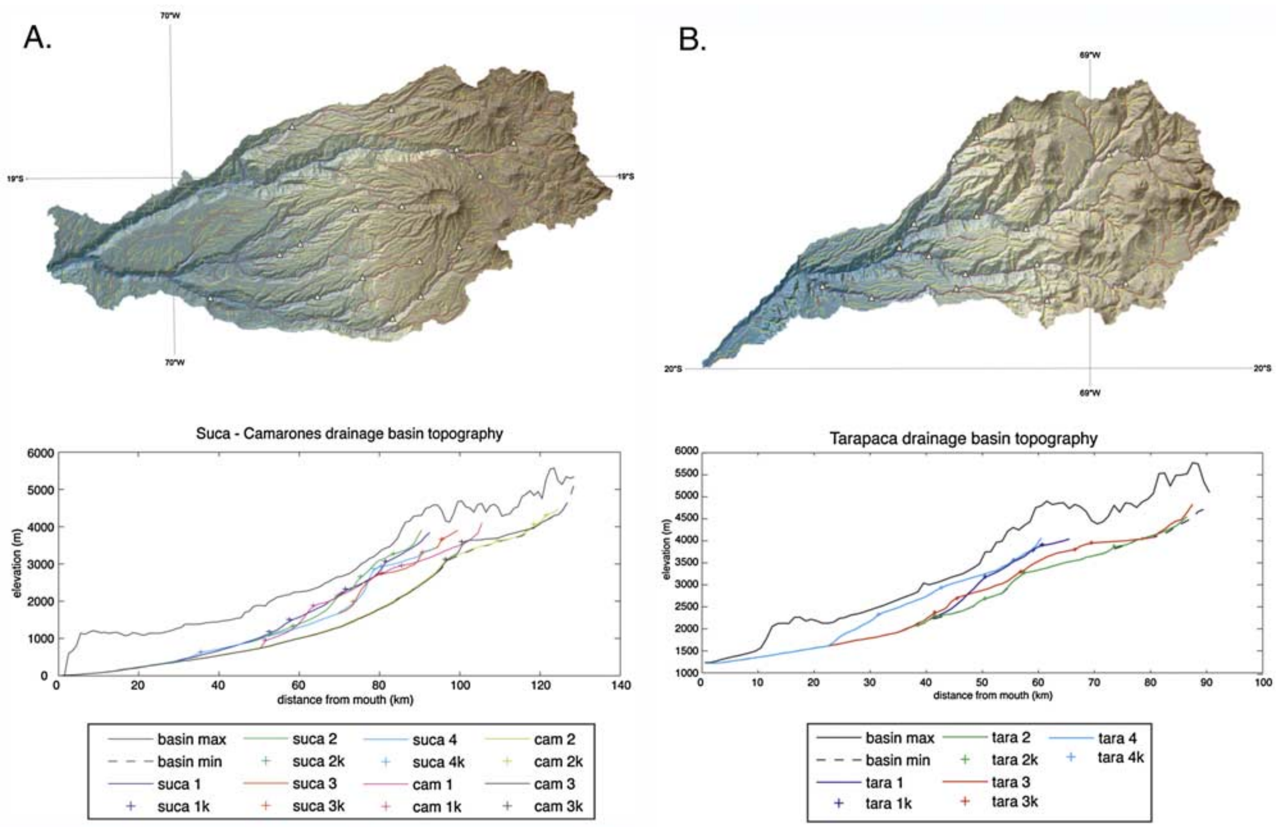

Figure 5. Shaded relief topography, drainage networks, and swath topographic profiles showing the relief structure of basins that drain the western mountain front into the Pacific Ocean (Figure 5a) and the effectively closed Pampa del Tamarugal Basin (Figure 5b). Knickpoints are marked by yellow triangles. (a) Río Camarones–Quebrada Suca catchment with trunk stream and tributaries (colored profiles) from the Río Camarones (''cam'') and the Quebrada Suca (''suc'') plotted with the maximum and minimum topography for a 70 km wide swath (black profiles) running along the basin axis. (b) Quebrada Tarapacá catchment with trunk and tributaries (colored profiles) plotted with the maximum and minimum topographic envelopes (black profiles) for a 47 km wide swath. All river profiles were projected into the line used to create the swath profiles. Minimum and maximum topographic profiles are determined by selecting the maximum and minimum cell values for each 1 km step length in the swath profiles. Note that the Tarapacá profiles end in the Central Depression and do not outlet to sea level.

of the long profile of a steady state river given by *Whipple and Tucker* [1999]:

$$x(x) = z_0 - (U/K)^{1/n}\left(1 - \frac{hm}{n}\right)^{-1}\left(x_0^{1-hm/n} - x^{1-hm/n}\right) \qquad (4)$$

where x_0 and z_0 are the position and elevation at the top of the profile, respectively. The power law relationship in (3) is observed directly in stream profiles extracted from digital elevation models, and the parameters m/n and $(U/K)^{1/n}$ can be derived by a regression through slope-area data. The ratio m/n (slope of the regression line) is commonly referred to as the concavity index (θ), while $(U/K)^{1/n}$ (slope intercept) is the steepness index (k_s). The values of k_s and θ are highly correlated; therefore we report values for k_s that are normalized (k_{sn}) to a reference concavity $\theta = 0.4$, a value in the range of those commonly reported [*Snyder et al.*, 2000]. Concavity values for the rivers considered in this study range between 0.15 and 20, which is much greater than the theoretical range of 0.3 to 0.6 [*Hack*, 1957; *Snyder et al.*, 2000, and references therein]. As discussed by *Whipple* [2004], such very high concavities are (1) usually local to short reaches of rivers and (2) often indicative of disequilibrium river profiles. An alternative explanation for this concavity range could be the strong contrast between different rock types.

[15] River long profiles are thought to represent the relief structure of the landscape [*Whipple et al.*, 1999; *Whipple and Tucker*, 1999], therefore knickpoint-bounded profile segments are transient pieces of a profile that represent some prior set of relief conditions. Whether relief is generated through base level fall in the downstream end or uplift of the headwaters, a perturbation in the relief

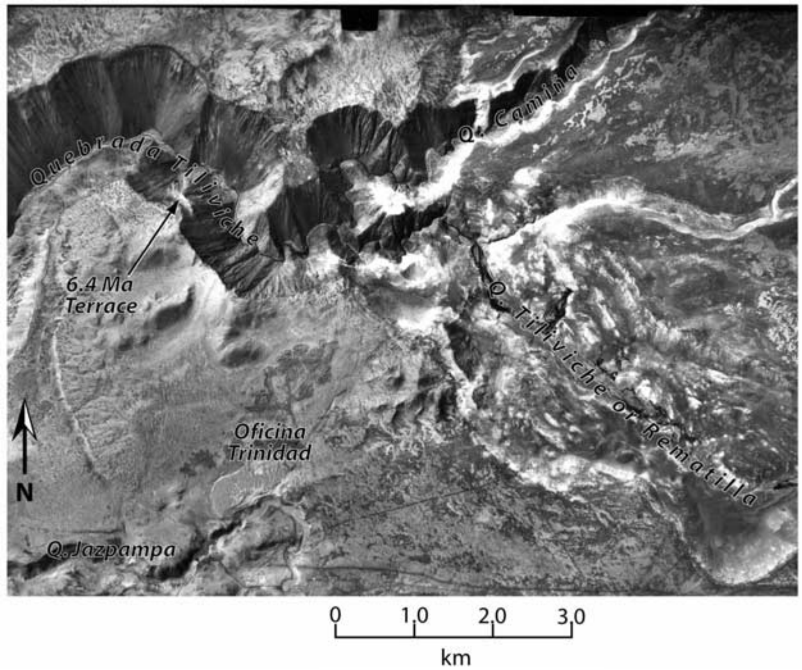

Figure 6. Aerial photo showing the location of the strath terrace preserved in the Quebrada Tiliviche canyon, downstream from the confluence of the Quebradas Camiña and Rematilla. U-Pb dating of zircons in an ash preserved on the terrace yields an age of ~6.4 Ma (see auxiliary material Text S1).

structure is produced. In northern Chile, base level remained nearly fixed during the period between 10 and 5.4 Ma, as evidenced by the incision of Quebrada Tiliviche in the north and the closed/effectively closed Pampa del Tamarugal to the south, while the total relief for the basins draining the western slope changed because of uplift. Each profile segment reflects different relief conditions and therefore can be used to estimate the amount of relief generated between the knickpoint bounded segments [i.e., *Clark et al.*, 2005]. Knickpoints or broader knick zones are discontinuities in river profiles that can be large or small and generally are introduced into a profile by a perturbation in either side of equation (1). The perturbations may be either a change of erosion rate (through climate change), or a change in downstream slope caused by adjustment to a new base level through capture or breakthrough, or a change in upstream slope caused by tectonic uplift or subsidence. Conceptually, tectonic uplift can be viewed as a relative base level fall. Irrespective of the ultimate cause, knickpoints create anomalous zones of increased slope that result in focused erosion. According to *Whipple and Tucker* [1999], knickpoints should migrate upstream as a wave from their point of origin. The section of the stream that lies upstream from the knickpoint operates under the same set of conditions as before, while points downstream of the knickpoint have adjusted to a new equilibrium profile. In areas where the channel incision rate (ε) is low, the propagation of the knickpoint wave upstream through the profile may be sufficiently slow that it can be observed and measured. Here we surmise that the conditions in northern Chile favor the slow upstream propagation of knickpoints.

[16] The river profile data presented here were extracted from Shuttle Radar Topography Mission (SRTM) digital topography corrected for data dropouts using a linear interpolation scheme. Fortunately the SRTM data for this region do not contain large (>0.5 km^2) zones of data dropout. Large flat areas constituting salars (salt pans) were removed from the topographic data using the mapped distribution of salars from a 1:1,000,000 scale geologic map of Chile [*SERNAGEOMIN*, 2002] prior to the extraction of directional and area accumulation grids. Individual drainage basins were identified and extracted from the larger grids of area and elevation for analysis. Because two different classes of drainage basins exist in our study area, two separate sets of criteria were used to extract drainage basins from the topographic data. In the region where rivers drain into the Pampa del Tamarugal Basin (19.5°−22°), outlets were picked at alluvial fan heads, which generally mark the transition between the alluvial (depositional) and confined (net erosional) segments of the rivers. Drainage basins that reach the Pacific Ocean were assigned outlets at sea level. River profiles were extracted from these data and analyzed following the procedures outlined by *Wobus et al.* [2006]. Because of the medium spatial resolution of the topographic data, the minimum area cutoff used for river profiles was 121 grid cells or 0.98 km^2. The elevation data for each profile were binned in 30-m increments, mildly filtered with an algorithm that removes artificial spikes in the data and smoothed with a 500 m

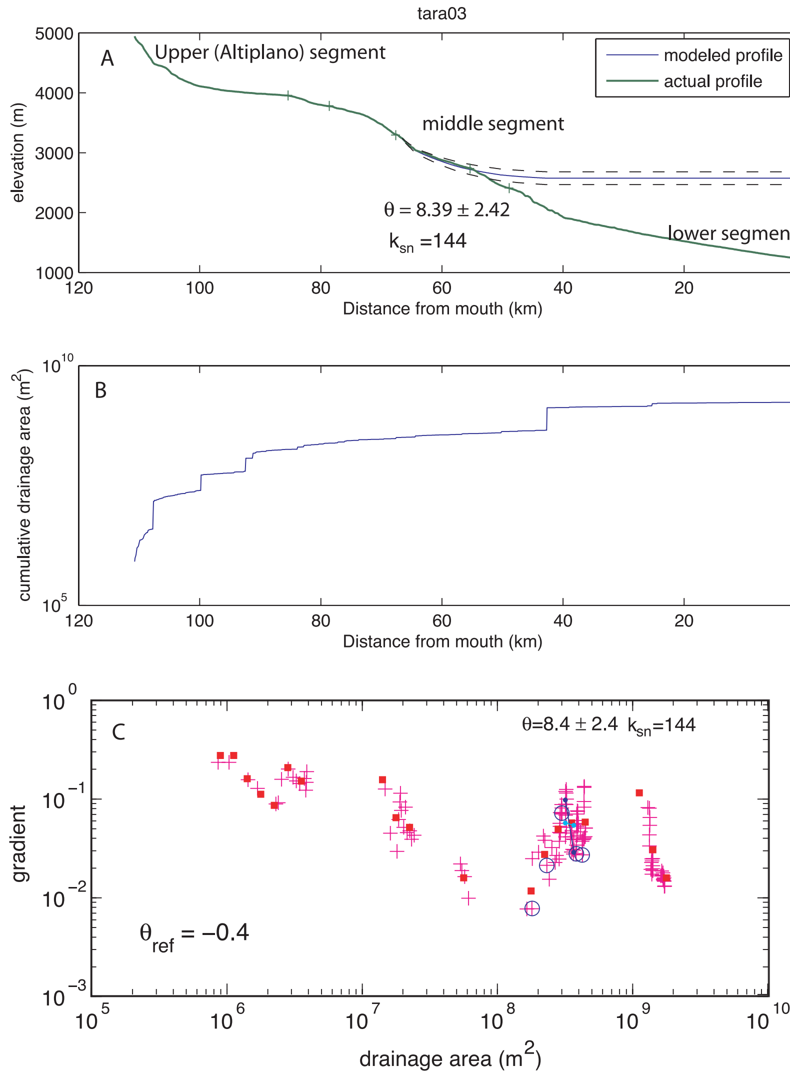

Figure 7. An example of a stream long profile from the Tarapacá basin with three distinct concave profile segments that are bounded by zones of strong convexities. (a) Stream long profile with the downstream projection of the middle stream segment. The different stream segments are labeled accordingly. (b) Graph showing cumulative drainage area with distance downstream. (c) Plot of stream gradient versus cumulative drainage area for the same stream. The concavity and k_s values for the modeled stream segment in Figure 7a were derived by the linear regression of slope-area data that corresponds to that stretch of the stream (dark blue line). Purple crosses show the slope data corresponding to 30 m elevation bins, while the red squares show a log binning of the same data.

(horizontal) moving window [*Wobus et al.*, 2006]. In most cases, longitudinal profiles and plots of slope vs. area were examined for several tributaries in each drainage basin. Knickpoints and other profile discontinuities were mapped on the profiles. The parameters used to model individual stream segments, the steepness index (k_{sn}) and concavity index (θ), were derived from regression of channel slope versus cumulative drainage area in log-log space. While we apply the methods presented above, particularly equations (3) and (4) to project the stream segments, we find it necessary to point out that the end result would likely vary very little from results obtained by the application of a simple power law curve fitting to the profile segments.

5. Results

[17] The rivers that drain the western Andean mountain front exhibit a wide variety of profile forms (e.g., Figures 5 and 7), but generally have at least 2 and often 3 distinct concave-up knickpoint-bounded segments, an upper, middle and lower (Figure 5). The river segments studied here are broadly similar in form to those of *Schoenbohm et al.*'s

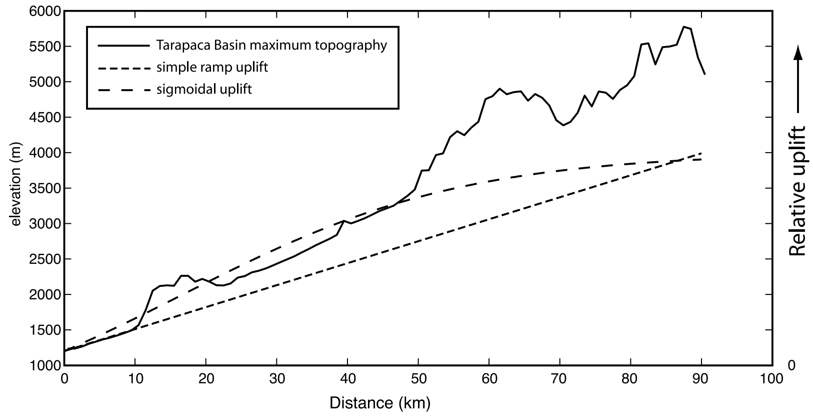

Figure 8. Different uplift models (dashed lines) plotted against the maximum topography of the Tarapacá Basin (solid line). The uplift models represent the total uplift of the plateau relative to the Central Depression (~25 Ma to Present). Since so little erosion has occurred on the western Andean mountain front over the last 10 Ma, the present topography serves as an approximation for uplift as a function of distance from the Central Depression, $U(x)$.

[2004] study of tributaries draining into the Red River in China. Lower segments reflect either the modern transition between alluvial fans and confined channels in the Pampa del Tamarugal (Figures 5b and 7) or the Pacific Ocean (Figure 5a). Middle segments are generally steeper and can contain linear segments and broad convex knick zones marking their upper limits; the highest concavity index and k_s values are found in these segments. The upper segments almost universally fall within the "typical" range of the concavity index (see discussion above) with values between 0.15 and 1.0.

[18] For reasons detailed in the three paragraphs that follow, we attribute the generation of knickpoints on the western slope to be the result of tectonic uplift of the western Andean mountain front and adjacent Altiplano, rather than the result of climate change or sudden base level fall related to breakthrough of streams to the Pacific Ocean (see below) or relative subsidence of the Pampa del Tamarugal Basin. The generation of knickpoints remains controversial, since it involves many factors related to lithology (K in equation (1)), climate (K in equation (1)) and uplift (U in equation (1)) and how these factors contribute to channel form. It is possible that knickpoints or waves of erosion generated in part of the profile where the rock is easily eroded could accumulate spatially on more resistant lithologies creating broader knick zones.

[19] Since the climate of northern Chile has been generally arid to hyperarid since the middle Miocene [*Alpers and Brimhall*, 1988; *Rech et al.*, 2006; *Sillitoe and McKee*, 1996], we reason that the episodic nature of precipitation that accompanies arid conditions has not changed in a way that would result in significant profile modification (i.e., knickpoint generation), although it is difficult to rule out entirely. While climatic fluctuations have been detected regionally [*Betancourt et al.*, 2000; *Bobst et al.*, 2001; *Latorre et al.*, 2002; *Rech et al.*, 2002], *Rech et al.* [2006] argue that time averaged precipitation did not exceed 200 mm/yr for the entire area. In this part of northern Chile there are streams that outlet to the Pacific Ocean and those that are effectively closed basins, yet both classes of streams contain prominent knickpoint-bounded segments and prominent knick zones (Figure 5). For many catchments that drain into the Pacific Ocean, the wave of erosion has migrated back substantially in the trunk streams, but this wave has not propagated through all of the tributaries (Figure 5a "cam2" and "cam 3" trunk stream profiles, compared with the "cam1" profile and the suca profiles).

[20] Surface uplift of the western mountain front and Altiplano Plateau relative to the Central Depression would not occur as a uniform step function all across the region being uplifted, but rather as a ramp function or a sigmoidal function (Figure 8). This logic follows from the common observation that crustal thickness varies laterally in a continuous manner, thus the amount of uplift should decrease smoothly toward the unthickened crust of the fore arc potentially resulting in a ramped or sigmoidal shape. Either function would result in a rotational steepening of the catchment. Despite this deviation from the step function assumed by *Whipple and Tucker* [1999] and *Snyder et al.* [2000], the end result of "relative base level fall" related to the uplift should be the same and induce the formation of a knickpoint that allows its catchment to readjust to its new base level. *Kirby and Whipple* [2001] improved upon the step function models initially presented by *Whipple and Tucker* [1999] and modeled the evolution of channel profiles by using a simple power law uplift function. In the case where the exponent was negative, and uplift decreased away from the headwaters, the concavity (θ) values were high (>1). If uplift increased away from headwater regions, the concavity values were low and even negative (forming convexities) in some cases. In general, stream segments in the lower and middle parts of the northern Chilean streams considered here have (θ) values >1, suggesting a decreasing uplift rate to the west. The sigmoidal uplift function that is

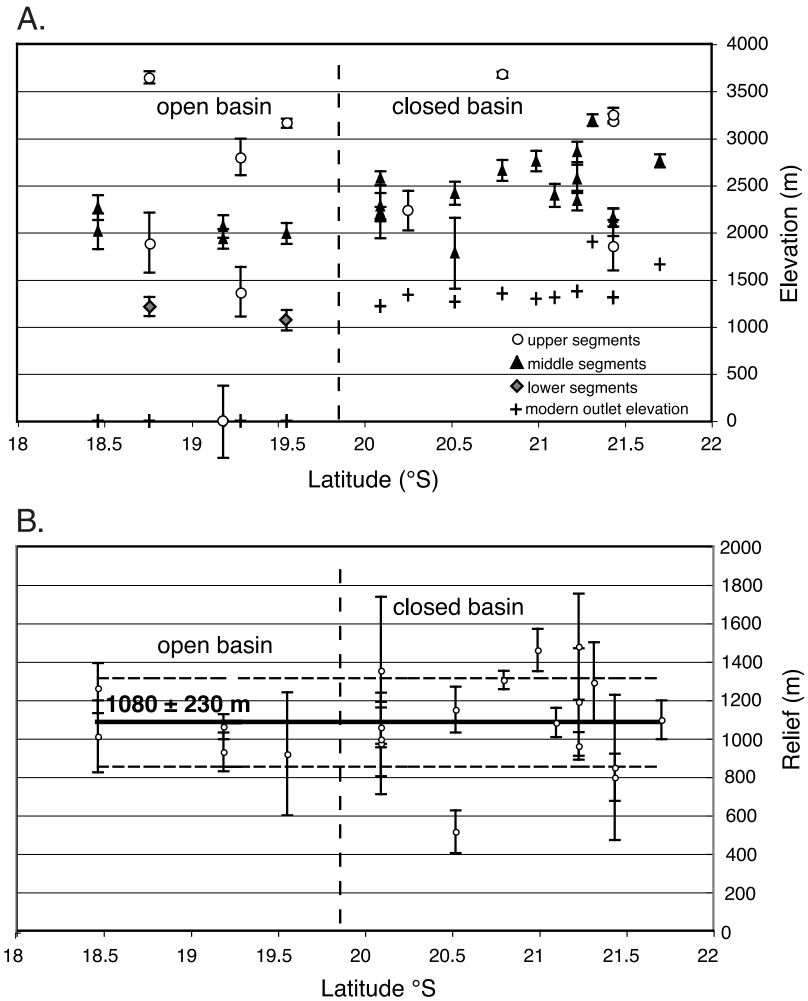

Figure 9. (a) Projected tributary outlet elevations for 34 streams in 15 catchments that drain the western slope and have well-defined knickpoint-bounded segments. Open circles correspond to upper knickpoint-bounded segments, solid triangles correspond to middle knickpoint-bounded segments, and solid diamonds are lower profile segment projections as described in Figure 7. The elevations of the modern outlets are marked by crosses, which are very similar in elevation to the lower segment projections for the rivers north of the effectively closed Tamarugal Basin. (b) Relief between modern river outlets and the elevation of the projected river segment outlets for 21 streams that have well-defined middle elevation knickpoint-bounded segments. Closed basin and corrected open basin relief values have an average of 1080 ± 230 m, which is interpreted here to represent tectonic uplift.

expected for the western Andean mountain front (Figure 8) has a near constant amount of uplift in the higher regions (east) that gently rolls over into a steep gradient in uplift rates toward the west before decreasing to zero. A simple numerical experiment using a stream power based model for which uplift conditions changed from an initial steady state profile, produced with a uniform uplift pattern, to a sigmoidal-shaped uplift pattern confirmed that a sigmoidal uplift pattern would indeed produce a knickpoint. Knickpoint generation occurred at the base of the profile outlet and migrated upstream producing a geometry similar to what we observe for the rivers of the western Andean slope.

[21] Assuming a tectonic origin for the knickpoint-bounded segments, we modeled the downstream projection of river longitudinal profiles using equation (4), as illustrated in Figure 7a, for a total of 34 knickpoint-bounded profile segments from 15 of the 20 catchments that drain the western slope (Figure 9a). The parameters (θ and k_{sn}) used to project the profiles are from linear regressions of the stream segments in slope-area plots (Table 1 and auxiliary material Text S2). The outlet elevations of the projected stream profiles (extended to the same horizontal position as the modern outlet) are between 0 m and 3672 m, inclusive of the profiles projected for lower, upper and middle stream segments (Figure 9a). Because the inferred uplift pattern for

Table 1. Projected Stream Outlet Elevations and Base Levels

Stream Segment	Outlet Latitude	Segment Type[a]	Concavity θ	k_{sn} $\theta = -0.4$	r^2	Outlet Elevation, m	Error, m	Base Level, m
aza003	−18.47	m	−0.70	53.0	0.84	2262	130	1000
aza006	−18.47	m	−0.58	74.0	0.90	2011	188	1000
vit201−1	−18.76	u	0.42	31.1	0.79	3645	65	1211
vit201−2	−18.76	l	2.10	111.0	0.82	1211	101	1211
vit202	−18.76	u	0.58	57.7	0.77	1891	320	1211
cam001	−19.19	u	0.39	46.9	0.81	1369	264	1000
cam003	−19.19	u	0.54	42.5	0.82	2798	194	1000
suc001−1	−19.19	u	0.25	53.2	0.75	−10	383	0
suc001−2	−19.19	m	2.50	94.6	0.75	1931	104	1000
suc003	−19.19	m	1.16	72.0	0.71	2062	119	1000
tili01−1	−19.55	m	10.30	212.0	0.79	1987	111	1067
tili01−2	−19.55	u	21.00	184.0	0.75	3158	48	1067
tili01−3	−19.55	l	5.10	77.2	0.83	1067	110	1067
tara02−1	−20.09	m	13.80	164.0	0.76	2194	76	1219
tara02−2	−20.09	m	3.60	192.0	0.47	2216	280	1219
tara03	−20.09	m	8.40	133.0	0.78	2574	72	1219
tara04	−20.09	m	0.66	44.0	0.53	2277	276	1219
quip03	−20.25	u	0.37	53.8	0.86	2231	209	1337
jmor01	−20.52	m	1.00	43.3	0.92	2414	123	1263
jmor04	−20.52	m	0.45	89.4	0.72	1778	378	1263
chac01	−20.80	m	1.00	56.3	0.70	2465	101	1353
chac07	−20.80	u	0.83	16.2	0.82	3672	32	1353
guat01	−20.99	m	1.20	87.6	0.70	2755	165	1295
mani01	−21.10	m	0.41	39.5	0.78	2392	121	1309
sup02a−1	−21.23	m	1.60	52.0	0.60	2566	149	1376
sup02a−2	−21.23	m	0.68	44.0	0.82	2337	106	1376
sup04	−21.23	m	0.76	64.5	0.82	2854	109	1376
viej01	−21.31	m	0.99	35.2	0.90	3191	63	1900
tamb01	−21.43	u	0.79	45.3	0.98	3251	72	1307
tamb02	−21.43	u	2.30	68.7	0.60	3206	98	1307
tamb03	−21.43	m	0.15	26.4	0.56	2105	289	1307
tamb04	−21.43	u	0.57	68.8	0.49	1864	267	1307
tamb04−2	−21.43	m	0.38	34.9	0.85	2157	97	1307
arc01	−21.70	m	0.65	24.9	0.94	2759	70	1661

[a]Segments are u, upper; l, lower; m, middle.

the western slope results in westward rotational steepening of the catchments, our modeled outlet elevations are minimum estimates.

[22] An especially interesting measure is the relief between the modeled paleoprofile outlet constructed for the middle segments of streams compared to the actual elevation of the modern outlet (Figure 9a). If tectonic forces are responsible for the relief generation, as we postulate here, then the difference between the outlets serves as a measure of uplift. When considering the measured relief, rivers that presently drain into the Pacific Ocean contain ~1 km more relief than the rivers that drain into the Pampa del Tamarugal Basin (difference in elevation between the crosses and triangles in Figure 9a). This difference in relief invites two different interpretations: either an additional kilometer of uplift has occurred in the area north of 19.75°S, or the projected middle segments of the northern streams formed relative to a base level equivalent to the elevation of the modern Central Depression, i.e., prior to whatever event caused the incision of the Coastal Cordillera and the Central Depression. In order to isolate the impact of tectonic uplift of the western slope, we subtract the relief generation caused by the incision event across the Coastal Cordillera. This correction for "Coastal Cordillera incision" is quantified as follows. Profiles from particularly inactive tributaries in two separate catchments that drain into the Pacific Ocean contain rivers with lower profile segments having downstream projections that result in outlet elevations of 1070 ± 110 m and 1200 ± 100 m. These elevations correspond with elevations of the El Diablo pediment surface that forms the broad flat interfluves between the canyons. The 1070–1200 m elevation range also corresponds to the outlet elevations for the modern streams that drain into the effectively closed Pampa del Tamarugal Basin to the south. In three northern drainages (Tiliviche, Suca-Camarones, and Vitor), we interpret these projections to represent the prior base level of the mountain front drainage system, before the streams equilibrated to the modern ~1000 m relief between the Pacific Ocean and the Central Depression. On the basis of the dated river terrace in the Quebrada de Tiliviche (see above), where it currently incises across the Coastal Cordillera, we interpret that the rivers to the north were graded to the Pampa del Tamarugal base level prior to ~6.4 Ma. The Río Azapa valley, which outlets where there is no Coastal Cordillera, was also graded to the now 1000 m high El Diablo surface, so we can apply

a similar correction to its projected stream segments. For basins where lower profile stream segments project near the closed basin paleobase level, that value was applied to correct for "Coastal Cordillera incision", otherwise the stream base level is set to 1000 m. Such a correction is not necessary for the closed basins south of the Quebrada Tiliviche, where no ambiguity exists regarding the lower river segment base level history.

[23] Applying the base level correction to the streams north of the modern Pampa del Tamarugal closed basin, the 21 modeled profiles that represent the middle segments have an average relief between the modeled paleoprofile outlet compared to the actual/corrected elevation of the modern outlet of 1080 ± 230 m (Figure 9b). We interpret the consistent clustering of relief over a 350 km long stretch of the western mountain front to represent tectonically generated relief related to the relative uplift of the western mountain front and adjacent central Andean Plateau with respect to the Central Depression.

[24] In the preceding we have assumed, for the sake of simplicity, that the elevations of the Coastal Cordillera and Central Depression have remained similar to their present values throughout the time of stream profile preservation. However, there are no constraints. While this does not affect the relative uplift interpretations for the modeled stream segments, it does leave alternative interpretations for the lower stream segments in the northern streams. Specifically, we cannot differentiate between a model where base level fell through drainage breakthrough of the Coastal Cordillera and a model where the northern streams persistently outlet to the ocean and ~1 km of wholesale uplift of the Coastal Cordillera and Central Depression occurred following 6.4 Ma [*García and Hérial*, 2005]. The lack of accommodation structures in the seismic data between the Central Depression and the western mountain front [*Digert et al.*, 2003] implies that should the latter model be true this uplift would also affect the elevations on the plateau.

[25] The modeled projections of the upper profile segments (11 profiles) have a wide range of projected outlet elevations, between −10 and 3675 msl (Figure 9a). This great scatter highlights the difficulty in deciphering the evolution of these highest stream segments with respect to the rest of the catchment. These parts of the stream network reach high in the Western Cordillera and Altiplano, where a long history of volcanic edifice construction and early Cenozoic deformation complicate the set of controls. There was a pervasive influence of middle Miocene to Pliocene volcanic activity as far south as 20°S, as well as the existence of prior mountainous relief related to the Incaic (Eocene-Oligocene) deformation in areas south of 20°S, each of which makes it difficult to ascertain whether or not the highest reaches of the profiles were always linked to their current trunk streams or are the result of more recent captures. Because it is uncertain that these upper stream segments evolved as part of their current catchment basin, we do not consider these upper river profile projections to be an accurate indicator of tectonic relief creation. The timing of uplift recorded in the middle stream segments can be inferred from the age of the stream segments modeled. As all middle segments dissect the 10 Ma (or 8.5–7.5 Ma proposed by *von Rotz et al.* [2005]) pediment surfaces that cap the El Diablo and Altos de Pica Formations, the modeled segments and their uplift must be younger than the pediment surface. The middle profile segments of suc003 and tili01a (Table 1) also deeply dissect (>500 m) the 8–9 Ma Tana lava [*Pinto et al.*, 2004] and underlying units, indicating that these modeled stream segments are younger than 8–9 Ma. Last, the middle profile segments of sup04, tamb03 and arc01 transect, with only tens of meters of incision, valleys that contain terraces built of alluvial gravels and the intercalated 5.4 Ma Carcote ignimbrite (Figure 4). In downstream areas of the same middle profile segments, the valleys contain strath terraces capped by Carcote ignimbrite high on the canyon walls [*Tomlinson et al.*, 2001]. We use the projection of the river profiles and the average elevations of areas mapped as Carcote by *Tomlinson et al.* [2001] as a means of evaluating the age of incision of the rivers (Figure 10). In the Quebrada Sipuca (Figure 10a), the elevation of the Carcote exposures corresponds well with the actual middle stream segment for sup04 and modeled downstream projection of the middle segment between 40 and 33 km along the profile, then the Carcote terraces decrease sharply in elevation (33 to 26 km in Figure 10a inset). We interpret the Carcote Ignimbrite capped terraces between ~36 km and 26 km to reflect the paleostream profile at 5.4 Ma. Clearly, incision of the middle segment was well under way in the Quebrada Sipuca by 5.4 Ma and suggests that surface uplift had to have occurred before deposition of the Carcote ignimbrite. The correspondence between the elevation of the Carcote remnants and the modeled middle segment are consistent with an interpretation in which the lower profile knickpoint erosional wave has deeply dissected the lower profile segments and is currently working on the downstream limit of the uplifted middle profile segments. Furthermore the correspondence of the modeled stream profile with the now stranded exposures of Carcote Ignimbrite confirm the validity of the profile modeling approach applied here. Despite similar occurrences of the Carcote in the Quebrada Tambillo (tamb03) and the Quebrada Arcas (arc01) profiles, not enough of the downstream extent of the ignimbrite terraces is preserved to allow for similar observations (Figures 10b and 10c). The timing of uplift is similar in age, and perhaps contemporaneous with the 6.4 Ma age of down cutting of the northern rivers to the ocean deduced from relations in the Quebrada Tiliviche. As the persistence of profile segments depends heavily on the rate of headward propagation of the knick zones, the suggestion is that the rate of propagation must have been slow, as evidenced by the slight advance of the Quebrada Tiliviche knick zone over the last 6.4 Ma [*Hoke*, 2006] and the 3 km of retreat since 5.4 Ma in the Quebrada Sipuca.

6. Discussion

[26] Our data show clear evidence for at least 1 km of surface uplift of the western Andean mountain front with respect to the Central Depression during the last 10 Ma.

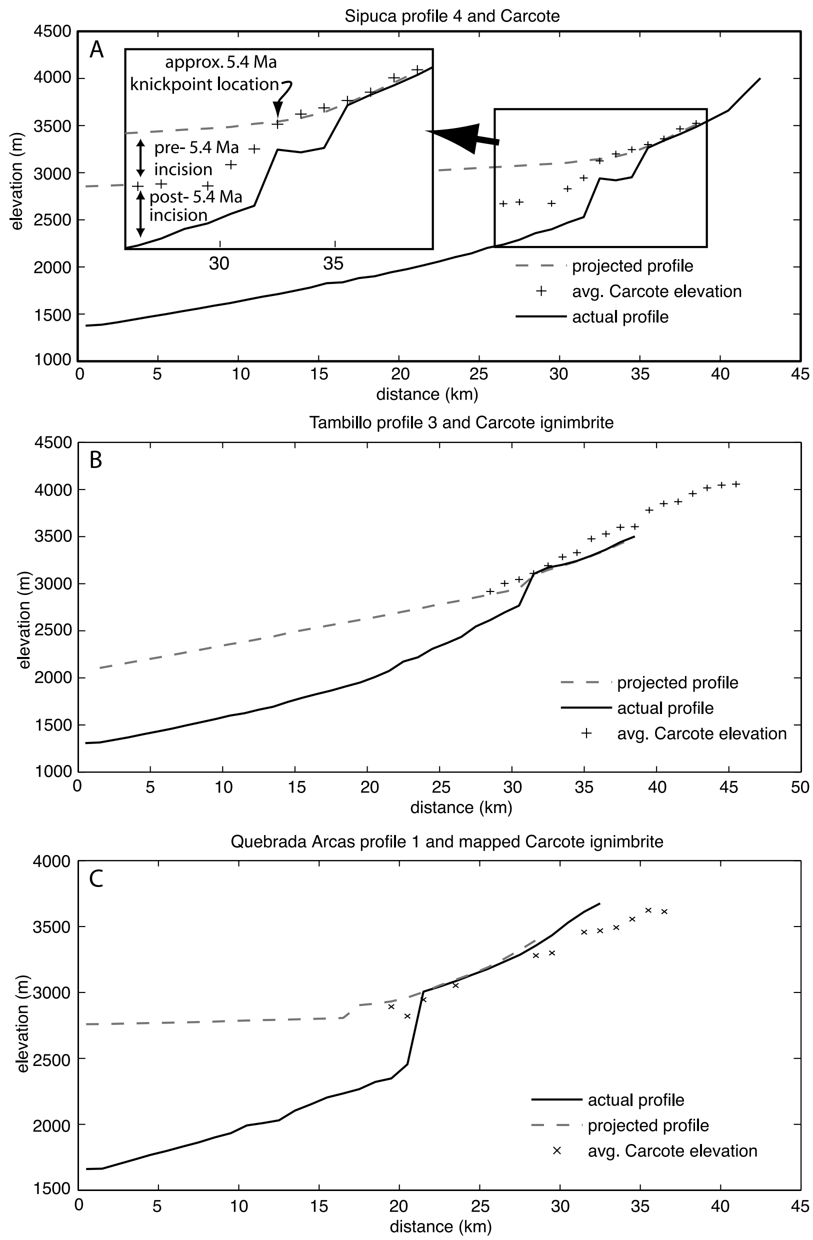

Figure 10. Relationship between the 5.4 Ma Carcote ignimbrite, the modeled middle river segments, and the actual river profile for sup04, tamb03 and arc01. The profiles, modeled and actual, and the average elevation of mapped outcrops of Carcote ignimbrite were projected into one straight profile line for each catchment. (a) The sup04 river profile showing that the Carcote ignimbrite is at similar elevations to the knickpoint-bounded middle segment and its modeled projection until ~33 km along the profile where it drops in elevation to a position between the modern profile and the modeled profile. (b and c) The tamb03 and arc01 modern and projected river profiles and the average elevations of the mapped exposures of Carcote ignimbrite. Less extensive deposition or exposure of the ignimbrite makes the interpretation more difficult, but the initial modeled segments and the mapped distribution of the Carcote correspond well with one another.

This result is unambiguous between 19.75° and 22°S where the streams drain to the modern closed Pampa del Tamarugal basin. In the area spanning 18.5°–19.75°S we reach this conclusion after subtracting ~1000 m for the base level change between the El Diablo–Altos de Pica surface and the modern river outlets to the Pacific Ocean. This is an important new constraint that tests *Isacks*' [1988] hypothesis of passive surface uplift of the western Andean slope and *Muñoz and Charrier*'s [1996] and *Victor et al.*'s [2004] model of upper crustal fault control on the western mountain front. Our data can only track the creation of increased relief, and not absolute elevation change, because the absolute elevation of our reference datum, the Central Depression, is not constrained. However, the 100s of meters of incision of the El Diablo surface in the Lluta and Azapa valleys near the coast, where the Coastal Cordillera is absent, would suggest that some uplift of the coastal region may have occurred within the last 10 Ma.

[27] The dynamics of the uplift model proposed by *Isacks* [1988] call for the formation of the western mountain front to be controlled by thermal and mechanical weakening of the South American lithosphere, due to subduction zone processes. In the model, the location of the mountain front coincides with the boundary between strong and weak lithosphere, which in turn coincides with the western tip of the asthenospheric wedge under the South American lithosphere [*Isacks*, 1988]. The model proposes a first phase of uplift to be the consequence of widespread horizontal shortening and crustal thickening during the "Quechua" phase of deformation. In the second stage of the model, when upper crustal deformation shifts eastward and the eastern foreland fold-and-thrust belts develop, the plateau grows higher in response to lower crustal ductile shortening and thickening driven by addition of mass from the underthrusting of the Bolivian foreland [*Isacks*, 1988]. The timing of the initiation of the second stage of deformation was refined by *Allmendinger et al.* [1997] to be 12 to 6 Ma. The cessation of deformation in the Eastern Cordillera was at ~10 Ma with earliest deformation in the Sub-Andean fold-and-thrust belt occurring as early as 9 Ma [*Echavarría et al.*, 2003]. *Isacks*' [1988] model treats the western Andean mountain front as a passive consequence of uplift and monoclinal tilting, driven by the tectonics within and east of the plateau.

[28] In contrast, the faulting models of *Muñoz and Charrier* [1996] and *Victor et al.* [2004] suggest that the uplift of the western mountain front can be explained solely by displacements on a west verging fault system that is exposed discontinuously from 18°30′S to ~21°30′S [*Digert et al.*, 2003; *García*, 2002; *García et al.*, 2004; *Muñoz and Charrier*, 1996; *Victor et al.*, 2004]. Throughout the system of faults and fault-related folds, the ages of unconformities, growth folds and syntectonic conglomerates indicate deformation is pre-6 Ma, with the greatest shortening rates constrained to be older than 10 Ma [*García et al.*, 2004; *García and Hérial*, 2005; *Pinto et al.*, 2004; *Victor et al.*, 2004]. Only minor post-6 Ma faulting and folding (<100 m displacement) occurs [*García et al.*, 2004; *Pinto et al.*, 2004]. For example, the modeled middle segments of stream profiles suc003 and tili01a (Table 1) lie east of the Moquella flexure, a 4 km wide growth fold [*Pinto et al.*, 2004]. *Pinto et al.* [2004] document ~650 m of uplift across the Moquella flexure between 25 Ma and the deposition of the 8–9 Ma Tana Lava but only 50 m of uplift younger than 8–9 Ma. The modeled stream segments crosscut and therefore postdate the Tana Lava, but the 50 m of uplift by post-Tana flexural folding is insufficient to explain the ~1 km of uplift indicated by the projected stream profile outlets.

[29] Shortening between 25 and 10 Ma along the western mountain front [*García et al.*, 2004; *García and Hérial*, 2005; *Pinto et al.*, 2004; *Victor et al.*, 2004] is compatible with both *Isacks*' [1988] first stage of plateau growth and the faulting models of *Muñoz and Charrier* [1996] and *Victor et al.* [2004], but the two models depart in regards to their predictions for the post-10 Ma uplift history. With the paucity of post-10 Ma fault activity on the west flank of the plateau [*Elger et al.*, 2005; *Victor et al.*, 2004], the upper crustal faulting model implies that significant uplift of the western edge of the plateau did not continue into the late Miocene. This prediction is contradicted by paleoelevation estimates from paleobotanical and stable isotope studies of paleosols which indicate large amounts of young uplift of the plateau, with more than 50% of the plateau elevation being attained in the last 10 Ma [*Garzione et al.*, 2006; *Ghosh et al.*, 2006; *Gregory-Wodzicki*, 2000; *Rech et al.*, 2006]. The early uplift requisite of the faulting model is also incompatible with the geomorphic results presented herein and other geomorphic studies which likewise indicate important post-10 Ma uplift [*Barke and Lamb*, 2006; *Gubbels et al.*, 1993; *Hoke et al.*, 2004; *Kennan et al.*, 1997; *Schildgen et al.*, 2007; *Worner et al.*, 2002] Another important distinction between *Isacks*' [1988] model and *Muñoz and Charrier*'s [1996] and *Victor et al.*'s [2004] model is their degree of consistency with isostatic compensation. Since the ratio of positive topography to continental root is ~1:5 [*Lowrie*, 1997], the 3–3.5 km of Neogene relief generation postulated for the central Andean Plateau requires ~20 km of Neogene crustal thickening. This value is in agreement with Eocene and current crustal thickness estimates under the western mountain front. Geochemical proxy data suggest that following Eocene magmatism and the Incaic shortening event, crustal thicknesses were ~45 km at 35 Ma [*Haschke and Gunther*, 2003; *Haschke et al.*, 2002], whereas geophysical data determine its current thickness to be 65–70 km [*Beck et al.*, 1996; *Wigger et al.*, 1994]. Shortening estimates from balanced cross sections along the western mountain front and western edge of the plateau (Western Cordillera) indicate 3 to 8 km of horizontal shortening that produces ~3–7 km of crustal thickening, far less than is required to explain the thickened Neogene crustal root. Since most of the shortening along the western mountain front occurred between 25 and 10 Ma, it would have been an important contribution to topographic development along the western edge of the central Andean Plateau during the early and middle Miocene, in accordance with both stage 1 of Isacks' model and the fault uplift model. However, the timing relationships clearly reveal that significant uplift of the central Andean Plateau younger than 10 Ma cannot be caused by the west vergent faults in northern Chile.

[30] We clearly document that uplift persisted into the latest Miocene. In this respect, our results provide evidence in support of *Isacks*' [1988] model for the uplift of the Altiplano. Specifically, we demonstrate that uplift of the western flank of the plateau continued as the eastern extent of Andean crustal shortening shifted eastward into what is now the Sub-Andean fold-thrust belt. The paucity of sig-

nificant post-10 Ma faulting activity in our study area suggests that ~1000 m of late Miocene uplift accompanied a lithospheric phenomenon that is not associated with local faulting and folding. Two likely candidates are lower crustal flow of material from the east in response to upper crustal shortening in the Sub-Andean fold-thrust belt and underthrusting of the Brazilian shield [*Isacks*, 1988], or removal of a dense lower crust and/or lithospheric mantle [*Garzione et al.*, 2006; *Kay and Kay*, 1993]. Mounting evidence exists in support of both of these mechanisms in the generation of continental plateaus [e.g., *Clark and Royden*, 2000; *Kay et al.*, 1994]. Our results are consistent with elevation increase since 10 Ma, and so are consistent with the paleoelevation estimates of *Gregory-Wodzicki* [2000] and *Rech et al.* [2006]. Our evidence for post-10 Ma uplift is similar to the timing of uplift suggested by *Garzione et al.* [2006] and *Ghosh et al.* [2006]. Furthermore our results lend support to other geomorphic evidence that suggests uplift more recent than 10 Ma, most notably the incision of the San Juan del Oro surface [*Barke and Lamb*, 2006; *Gubbels et al.*, 1993; *Kennan et al.*, 1997; *Schildgen et al.*, 2007], and the tilting and dissection of the ~10 Ma Atacama Gravels south of 25°S [*Mortimer*, 1973; *Riquelme et al.*, 2003].

7. Conclusions

[31] Downstream modeling of knickpoint-bounded stream segments on the western Andean mountain front reveal an ~1 km increase in relief, and landform relationships to dated strata indicate that the timing of relative uplift was within the last 10 Ma. Previous models for northern Chile calling upon only involvement of local deformation predicted the uplift of the plateau to have been nearly complete by the end of the middle Miocene. The late Miocene relief documented herein was created in the absence of significant deformation (i.e., faulting or folding) in the area, suggesting that processes occurring in the lower crust (i.e., lower crustal flow) or upper mantle (lithospheric delamination) are responsible for the growth of the central Andean Plateau during this period. Our results confirm the presence and timing of the second stage of plateau growth advocated by *Isacks* [1988].

[32] **Acknowledgments.** This material is based upon work supported by the National Science Foundation under grant 0208130 to T.E.J. and B.L.I. and supported by NASA Headquarters under Earth System Science Fellowship grant NGT5-30461 to G.D.H. We thank Carlos Pérez de Arce (SERNAGEOMIN) for $^{40}Ar/^{39}Ar$ analysis of the biotites. Tectonics reviewers Kelin Whipple and Jon Pelletier provided feedback which helped to clarify our presentation of this material. Kelin Whipple and his research group helped acquaint G.D.H. with the stream profile analysis methods. Discussions with Carmala Garzione (University of Rochester) and Noah Finnegan (University of Washington/Cornell) improved the ideas presented here.

References

Allmendinger, R. W., T. E. Jordan, S. M. Kay, and B. L. Isacks (1997), The evolution of the Altiplano-Puna plateau of the central Andes, *Annu. Rev. Earth Planet. Sci.*, *25*, 139–174.

Alpers, C. N., and G. H. Brimhall (1988), Middle Miocene climatic-change in the Atacama Desert, northern Chile—Evidence from supergene mineralization at La-Escondida, *Geol. Soc. Am. Bull.*, *100*, 1640–1656.

Barke, R., and S. Lamb (2006), Late Cenozoic uplift of the Eastern Cordillera, Bolivian Andes, *Earth Planet. Sci. Lett.*, *249*, 350–367.

Beck, S. L., G. Zandt, S. C. Myers, T. C. Wallace, P. G. Silver, and L. Drake (1996), Crustal-thickness variations in the central Andes, *Geology*, *24*, 407–410.

Betancourt, J. L., C. Latorre, J. A. Rech, J. Quade, and K. A. Rylander (2000), A 22000-year record of monsoonal precipitation from northern Chile's Atacama Desert, *Science*, *289*, 1542–1546.

Bobst, A. L., T. K. Lowenstein, T. E. Jordan, L. V. Godfrey, T. L. Ku, and S. Luo (2001), A 106 ka paleoclimate record from drill core of the Salar de Atacama, northern Chile, *Palaeogeogr Palaeoecol*, *173*, 21–42.

Clark, M. K., and L. H. Royden (2000), Topographic ooze: Building the eastern margin of Tibet by lower crustal flow, *Geology*, *28*, 703–706.

Clark, M. K., G. Maheo, J. Saleeby, and K. A. Farley (2005), The non-equilibrium landscape of the southern Sierra Nevada, California, *GSA Today*, *15*, 4–9.

Digert, F. E., et al. (2003), Subsurface stratigraphy of the Neogene Tamarugal Basin, northern Chile, paper presented at X Congreso Geológico Chileno, Uni.de Concepción, Concepción, Chile.

Dunai, T. J., G. A. Gabriel López, and J. Juez-Larre (2005), Oligocene-Miocene age of aridity in the Atacama Desert revealed by exposure dating of erosion-sensitive landforms, *Geology*, *33*, 321–324, doi:10.1130/G21184.1.

Echavarría, L., R. Hernández, R. Allmendinger, and J. Reynolds (2003), Subandean thrust and fold belt of northwestern Argentina; geometry and timing of the Andean evolution, *AAPG Bull.*, *87*, 965–985.

Elger, K., O. Oncken, and J. Glodny (2005), Plateau-style accumulation of deformation: Southern Altiplano, *Tectonics*, *24*, TC4020, doi:10.1029/2004TC001675.

Evenstar, L., et al. (2005), Miocene-Pliocene climate change in the Peru-Chile Desert, paper presented at 6th International Symposium on Andean Geodynamics, Inst. de Rech. pour le Dév., Barcelona, Spain, 12–14 Sept.

Farías, M., R. Charrier, D. Comte, J. Martinod, and G. Hérail (2005), Late Cenozoic deformation and uplift of the western flank of the Altiplano: Evidence from the depositional, tectonic, and geomorphologic evolution and shallow seismic activity (northern Chile at 19°30′S), *Tectonics*, *24*, TC4001, doi:10.1029/2004TC001667.

Galli Olivier, C., and R. J. Dingman (1962), Cuadrángulos Pica, Alca, Matilla y Chacarilla, con un estudio sobre los recursos de agua subterranea, provincia de Tarapaca, *Carta Geol. Chile*, *3*(2–5), 125 pp.

García, M. (2002), Evolution Oligo-Miocene de L'Altiplano Occidental (Arc et Avant-Arc du Nord Chili, Arica): Tectonique, volcanisme, sédementation, géomorphologie et bilan érosion-sédimentation, Ph.D. thesis, 118 pp, Univ. Joseph Fourier, Grenoble, France.

García, M., and G. Hérial (2005), Fault-related folding, drainage network evolution and valley incision during the Neogene in the Andean Precordillera of northern Chile, *Geomorphology*, *65*, 279–300.

García, M., et al. (2004), Hoja Arica, Región de Tarapacá, Serv. Nac. de Geol. y Minería, Santiago, Chile.

Garzione, C. N., P. Molnar, J. C. Libarkin, and B. J. MacFadden (2006), Rapid late Miocene rise of the Bolivian Altiplano: Evidence for removal of mantle lithosphere, *Earth Planet. Sci. Lett.*, *241*, 543–556.

Ghosh, P., C. N. Garzione, and J. M. Eiler (2006), Rapid uplift of the Altiplano revealed through C-13-O-18 bonds in paleosol carbonates, *Science*, *311*, 511–515.

Gregory-Wodzicki, K. M. (2000), Uplift history of the central and northern Andes: A review, *Geol. Soc. Am. Bull.*, *112*, 1091–1105.

Gubbels, T. L., B. L. Isacks, and E. Farrar (1993), High-level surfaces, plateau uplift, and foreland development, Bolivian central Andes, *Geology*, *21*, 695–698.

Hack, J. T. (1957), Studies of longitudinal stream profiles in Virginia and Maryland, U.S. Geol. Surv., Reston, Va.

Haschke, M., and A. Gunther (2003), Balancing crustal thickening in arcs by tectonic vs. magmatic means, *Geology*, *31*, 933–936.

Haschke, M., W. Siebel, A. Günther, and E. Scheuber (2002), Repeated crustal thickening and recycling during the Andean orogeny in north Chile (21°–26°S), *J. Geophys. Res.*, *107*(B1), 2019, doi:10.1029/2001JB000328.

Hoke, G. D. (2006), The influence of climate and tectonics on the geomorphology of the western slope of the central Andes, Chile and Peru, Doctoral thesis, 283 pp, Cornell Univ., Ithaca, N. Y.

Hoke, G. D., B. L. Isacks, T. E. Jordan, and J. S. Yu (2004), Groundwater-sapping origin for the giant quebradas of northern Chile, *Geology*, *32*, 605–608.

Houston, J., and A. J. Hartley (2003), The central Andean west-slope rainshadow and its potential contribution to the origin of hyper-aridity in the Atacama desert, *Int. J. Climatol.*, *23*, 1453–1464.

Isacks, B. L. (1988), Uplift of the central Andean Plateau and Bending of the Bolivian Orocline, *J. Geophys. Res.*, *93*, 3211–3231.

Jordan, T. E., J. H. Reynolds, and J. P. Erikson (1997), Variability in age and initial shortening and uplift in the central Andes, in *Tectonic Uplift and Climate Change*, edited by W. F. Ruddiman, pp. 41–61, Plenum Press, New York.

Kay, R. W., and S. M. Kay (1993), Delamination and delamination magmatism, *Tectonophysics*, *219*, 177–189.

Kay, S. M., et al. (1994), Young mafic back arc volcanic-rocks as indicators of continental lithospheric delamination beneath the Argentine Puna Plateau, central Andes, *J. Geophys. Res.*, *99*, 24,323–24,339.

Kennan, L., et al. (1997), High-altitude paleosurfaces in the Bolivian Andes: evidence for late Cenozoic surface uplift, in *Paleosurfaces: Recognition, Reconstruction and Paleoenvironmental Interpretation*, edited by M. Widdowson, *Geol. Soc. Spec. Publ.*, *120,* 307–323.

Kiefer, E., M. J. Dörr, H. Ibbeken, and H.-J. Götze (1997), Gravity-based mass balance of an alluvial fan giant: The Arcas Fan, Pampa del Tamarugal, northern Chile, *Rev. Geol. Chile*, *24*, 165–185.

Kirby, E., and K. Whipple (2001), Quantifying differential rock-uplift rates via stream profile analysis, *Geology*, *29*, 415–418.

Kober, F., et al. (2006), Surface uplift and climate change: The geomorphic evolution of the Western Escarpment of the Andes of northern Chile between the Miocene and present, in *Tectonics, Climate and Landscape Evolution*, edited by S. D. Willett et al., *Spec. Pap. Geol. Soc. Am.*, *398*, 75–86.

Lamb, S., and L. Hoke (1997), Origin of the high plateau in the central Andes, Bolivia, South America, *Tectonics*, *16*, 623–649.

Latorre, C., J. L. Betancourt, K. A. Rylander, and J. Quade (2002), Vegetation invasions into absolute desert: A 45000 yr rodent midden record from the Calama-Salar de Atacama basins, northern Chile (lat 22°–24°S), *Geol. Soc. Am. Bull.*, *114*, 349–366.

Lowrie, W. (1997), *Fundamentals of Geophysics*, 1st ed., 354 pp., Cambridge Univ. Press, Cambridge, U. K.

McQuarrie, N. (2002), The kinematic history of the central Andean fold-thrust belt, Bolivia: Implications for building a high plateau, *Geol. Soc. Am. Bull.*, *114*, 950–963.

McQuarrie, N., B. K. Horton, G. Zandt, S. Beck, and P. G. DeCelles (2005), Lithospheric evolution of the Andean fold-thrust belt, Bolivia, and the origin of the central Andean plateau, *Tectonophysics*, *399*, 15–37, doi:10.1016/j.tecto.2004.12.013.

Montgomery, D. R., and E. Foufoula-Georgiou (1993), Channel network source representation using digital elevation models, *Water Resour. Res.*, *29*, 3925–3934.

Montgomery, D. R., G. Balco, and S. D. Willett (2001), Climate, tectonics, and the morphology of the Andes, *Geology*, *29*, 579–582, doi:10.1130/0091-7613(2001)029<0579:CTATMO>2.0.CO;2.

Mortimer, C. (1973), The Cenozoic history of the southern Atacama Desert, Chile, *J. Geol. Soc. London*, *129*, 505–526.

Mortimer, C. (1980), Drainage evolution in the Atacama Desert of northernmost Chile, *Rev. Geol. Chile*, *11*, 3–28.

Mortimer, C., and N. Saric Rendic (1975), Cenozoic studies in northernmost Chile, *Geol. Rundsch.*, *64*, 395–420.

Mortimer, C., E. Farrar, and N. Saric (1974), K-Ar ages from Tertiary lavas of the northernmost Chilean Andes, *Geol. Rundsch.*, *63*, 484–490.

Mpodozis, C., and V. Ramos (1989), The Andes of Chile and Argentina, in *Geology of the Andes and Its Relation to Hydrocarbon and Mineral Resources*, edited by G. E. Ericksen et al., pp. 56–90, Circum-Pac. Counc. for Energy and Miner. Resour., Houston, Tex.

Muñoz, N., and R. Charrier (1996), Uplift of the western border of the Altiplano on a west vergent thrust system, northern Chile, *J. S. Am. Earth Sci.*, *9*, 171–181.

Muñoz, N., and P. Sepulveda (1992), Estructuras compresivas con vergencia al oeste en el borde oriental de la Depresion Central, norte de Chile (19°15′S), *Rev. Geol. Chile*, *19*, 241–247.

Muzzio, J. G. (1986), Geologia de los cuadrángulos Caleta Camarones, Cuya, Punta Gorda, y Cerro Atajaña, I region, Chile: Informe de Avance, Serv. Nac. de Geol. y Minería, Santiago, Chile.

Muzzio, J. G. (1987), Geologia de los cuadrángulos Pisagua, Zapiga, Caleta Buena y Huara: informe de Advance Proyecto hoja Pisagua, 2 maps, scale 1:100000, Serv. Nac. de Geol. y Minería, Santiago, Chile.

Pinto, L., et al. (2004), Sedimentación sintectónica asociada a las estructuras néogeneas en la Precordillera de la zona de Moquella, Tarapacá (19°15′S, norte de Chile), *Rev. Geol. Chile*, *31*, 19–44.

Rech, J. A., J. Quade, and J. L. Betancourt (2002), Late Quaternary paleohydrology of the central Atacama Desert (lat 22°–24°S), Chile, *Geol. Soc. Am. Bull.*, *114*, 334–348.

Rech, J. A., B. S. Currie, G. Michalski, and A. M. Cowan (2006), Neogene climate change and uplift in the Atacama Desert, Chile, *Geology*, *34*, 761–764, doi:10.1130/G22444.1.

Riquelme, R., J. Martinod, G. Herail, J. Darrozes, and R. Charrier (2003), A geomorphological approach to determining the Neogene to Recent tectonic deformation in the Coastal Cordillera of northern Chile (Atacama), *Tectonophysics*, *361*, 255–275.

Sáez, A., L. Cabrera, A. Jensen, and G. Chong (1999), Late Neogene lacustrine record and palaeogeography in the Quillagua Llamara basin, central Andean fore-arc (northern Chile), *Palaeogeogr. Palaeoclimatol. Palaeoecol.*, *151*, 5–37, doi:10.1016/S0031-0182(99)00013-9.

Salas, R., et al. (1966), Geología y recursos minerales del departamento de Arica, provincia de Tarapacá, Serv. Nac. de Geol. y Minería, Santiago, Chile.

Schildgen, T., K. V. Hodges, K. X. Whipple, P. W. Reiners, and M. S. Pringle (2007), Uplift of the western margin of the Andean Plateau revealed from canyon incision history, southern Peru, *Geology*, *35*(6), 523–526, doi:10.1130/G23532A.1.

Schoenbohm, L. M., K. X. Whipple, B. C. Burchfiel, and L. Chen (2004), Geomorphic constraints on surface uplift, exhumation, and plateau growth in the Red River region, Yunnan Province, China, *Geol. Soc. Am. Bull.*, *116*, 895–909, doi:10.1130/B25364.1.

Servicio Nacional de Geología y Minería (SERNAGEOMIN) (2002), Mapa geológico de Chile, 3 sheets, Santiago, Chile.

Sillitoe, R. H., and E. H. McKee (1996), Age of supergene oxidation and enrichment in the Chilean porphyry copper province, *Econ. Geol. Bull. Soc.*, *91*, 164–179.

Silva, L. I. (1977), Hojas Pisagua y Zapiga, I Region, Inst. de Invest. Geol., Santiago, Chile.

Snyder, N. P., K. X. Whipple, G. E. Tucker, and D. J. Merritts (2000), Landscape response to tectonic forcing: Digital elevation model analysis of stream profiles in the Mendocino triple junction region, northern California, *Geol. Soc. Am. Bull.*, *112*, 1250–1263, doi:10.1130/0016-7606(2000)11220021250:LRTTFD>2.0.CO;2.

Tobar, A., et al. (1968), Cuadrángulos Camaraca y Azapa. Provincia de Tarapacá, 20 pp. and 22 maps, scale 21:50000, Inst. de Invest. Geol., Santiago, Chile.

Tomlinson, A. J., et al. (2001), Geología de la Precordillera Andina de Quebrada Blanca Chuquicamata, Regiones I y II [20°30′–22°30′], 444 pp. and 20 maps pp, Serv. Nac. de Geol. y Minería, Santiago, Chile.

Tosdal, R. M., A. H. Clark, and E. Farrar (1984), Cenozoic polyphase landscape and tectonic evolution of the Cordillera Occidental, southernmost Peru, *Geol. Soc. Am. Bull.*, *95*, 1318–1332.

Victor, P., O. Oncken, and J. Glodny (2004), Uplift of the western Altiplano plateau: Evidence from the Precordillera between 20° and 21°S (northern Chile), *Tectonics*, *23*, TC4004, doi:10.1029/2003TC001519.

von Rotz, R., F. Schlunegger, F. Heller, and I. Villa (2005), Assessing the age of relief growth in the Andes of northern Chile: Magneto-polarity chronologies from Neogene continental sections, *Terra Nova*, *17*, 462–471, doi:10.1111/j.1365-3121.2005.00634.x.

Whipple, K. X. (2004), Bedrock rivers and the geomorphology of active orogens, *Annu. Rev. Earth Planet. Sci.*, *32*, 151–185.

Whipple, K. X., and G. E. Tucker (1999), Dynamics of the stream-power river incision model: Implications for height limits of mountain ranges, landscape response timescales, and research needs, *J. Geophys. Res.*, *104*, 17,661–17,674.

Whipple, K. X., E. Kirby, and S. H. Brocklehurst (1999), Geomorphic limits to climate-induced increases in topographic relief, *Nature*, *401*, 39–43, doi:10.1038/43375.

Wigger, P., et al. (1994) Variation in crustal structure of the southern central Andes deduced from seismic refraction investigations, in *Tectonics of the Southern Central Andes*, edited by K.-J. Reutter et al., pp. 23–48, Springer-Verlag, Berlin, Germany.

Wobus, C. W., K. V. Hodges, and K. X. Whipple (2003), Has focused denudation sustained active thrusting at the Himalayan topographic front?, *Geology*, *31*, 861–864, doi:10.1130/G19730.1.

Wobus, C., et al. (2006), Tectonics from topography: procedures, promise and pitfalls, in *Tectonics, Climate and Landscape Evolution*, edited by S. D. Willett et al., *Spec. Pap. Geol. Soc. of Am.*, *398*, 55–74.

Worner, G., D. Uhlig, I. Kohler, and H. Seyfried (2002), Evolution of the West Andean Escarpment at 18°S (N. Chile) during the last 25 Ma: Uplift, erosion and collapse through time, *Tectonophysics*, *345*, 183–198, doi:10.1016/S0040-1951(01)00212-8.

Zaprowski, B. J., F. J. Pazzaglia, and E. B. Evenson (2005), Climatic influences on profile concavity and river incision, *J. Geophys. Res.*, *110*, F03004, doi:10.1029/2004JF000138.

N. Blanco and A. J. Tomlinson, Servicio Nacional de Geología y Minería, Av. Santa María 0104, Santiago, Chile.

G. D. Hoke, Department of Earth and Environmental Sciences, University of Rochester, 227 Hutchinson Hall, Rochester, NY 14627, USA.

B. L. Isacks and T. E. Jordan, Department of Earth and Atmospheric Sciences, Cornell University, Snee Hall, Ithaca, NY 14853, USA.

J. Ramezani, Department of Earth Atmospheric and Planetary Sciences, Massachusetts Institute of Technology, 54-1117, Cambridge, MA 02139, USA.